Current Biology, Vol. 14, 69–74, January 6, 2004, ©2004 Elsevier Science Ltd. All rights reserved. DOI 10.1016/j.cub.2003.12.027

A Potential Tension-Sensing Mechanism that Ensures Timely Anaphase Onset upon Metaphase Spindle Orientation

Srividya Rajagopalan, Andrea Bimbo, Mohan K. Balasubramanian, and Snezhana Oliferenko*
Temasek Life Sciences Laboratory
1 Research Link
The National University of Singapore
117604 Singapore
Republic of Singapore

Summary

The spindle orientation checkpoint (SOC) in fission yeast has been proposed to delay metaphase-to-anaphase transition when the spindle poles are misaligned with respect to the long axis of the cell. This checkpoint is activated in the absence of either an actomyosin division ring [1] or astral microtubules [2]. Although the SOC could be overridden in the absence of the transcription factor Atf1p, its mechanistic nature remained unclear. Here, we show that the SOC-triggered metaphase delay depends on a subset of the spindle assembly checkpoint (SAC) components Mph1p and Bub1p. Based on this finding and a detailed imaging of the spindle orientation process, we hypothesized that the spindle pole might contain proteins capable of sensing the achievement of spindle alignment. We identified the kendrin-like spindle pole body resident Pcp1p as a candidate molecule. A targeted mutation in its central domain specifically triggered the SOC in spite of the presence of oriented spindles, causing a metaphase delay that could be relieved in the absence of Mph1p, Bub1p, and Atf1p. Thus, Pcp1p might provide a link between the mechanical process of spindle alignment and the signal transduction that initiates anaphase.

Results and Discussion

A correct orientation of the metaphase spindle lies at the heart of many developmental decisions [3–5]. How do cells monitor an achievement of "correct" orientation and translate it into initiation of subsequent mitotic events? Work in budding yeast has uncovered mechanisms by which such signals can be generated in asymmetrically dividing cells [6–8]. However, virtually nothing is known about corresponding mechanisms in cells with symmetric division patterns. There is evidence for existence of a spindle orientation checkpoint (SOC) in the fission yeast *Schizosaccharomyces pombe* (*S. pombe*) that delays metaphase-to-anaphase transition until the spindle is approximately perpendicular to the actomyosin ring [1, 2].

Gachet et al. proposed that the SOC depended on some components of the MAP kinase cascade and was distinct from the spindle assembly checkpoint (SAC) [1]. Their conclusion was based on the fact that latrunculin B (latB)-treated *mad2*Δ cells engaged the SOC, in spite of the absence of the actomyosin ring [1]. They also asserted that destruction of both cyclin B (Cdc13p) and securin (Cut2p) in latB-treated wild-type cells occurred with normal kinetics, suggesting that the SOC did not involve inhibition of the anaphase-promoting complex (APC) [1]. Yet, we have previously shown that asterless *mia1*Δ cells, defective in spindle orientation, exhibited high Cdc13p levels throughout the metaphase delay [2].

Here, we assessed Cdc13p-YFP levels [9] in latrunculin A (latA)-treated cells by fluorescence microscopy. We utilized a temperature-sensitive *cdc25-22* mutant as a means to synchronize cells at the G2/M boundary in order to bypass the size-dependent mitotic entry checkpoint [10]. Experiments were performed as described in the Experimental Procedures section. We found that latA-treated Cdc13p-YFP *cdc25-22* cells delayed in metaphase for ~20 min, as compared to DMSO-treated control, with Cdc13p-YFP localizing to spindles, spindle pole bodies (SPBs), and nucleoplasm throughout the delay (Figures 1A and 1B). Similar results were obtained using 10 μM latA [10] and 10 μM latB [1] (Figures S1A and S1B). Using Cut2p-GFP [11] *cdc25-22* cells, we also found that securin levels remained unchanged during latA-induced metaphase block (Figures 1C and 1D). We concluded that the APC was inhibited and CDK activity remained high when SOC was activated.

We then checked whether the latA-induced metaphase delay could be abrogated in the absence of particular SAC components. After analyzing a panel of SAC deletion mutants, we concluded that Mph1p and Bub1p, but not Mad2p, Mad3p, and Bub3p, were involved in maintaining the delay (Figures 1E–1I). Strikingly, we also found that cells lacking Atf1p, the proposed effector for the SOC [1], were hypersensitive to low doses of the microtubule-destabilizing drug MBC, similar to the de facto SAC components' mutants (Figure 1J and data not shown). Thus, it is possible that alleviation of the SOC in *atf1*Δ cells might be the result of compromised SAC function. The role of the SAC in monitoring spindle orientation could not be determined using the asterless *mia1*Δ mutant [2] owing to compound problems in kinetochore attachment and spindle alignment in these cells [12, 13]. Our results so far indicated that the SOC was a facet of the SAC, since a subset of SAC components monitored metaphase spindle orientation.

What could be the nature of the signal that promotes anaphase upon spindle alignment? To get an insight into this process, we analyzed the dynamics of spindle orientation. We performed time-lapse analyses of mitotic cells simultaneously expressing α-tubulin-EGFP [14] and the actomyosin ring marker Rlc1p-EGFP [15, 16] (n = 25, Figure 2 and movie S1). As the spindle reached its full metaphase length and Rlc1p-EGFP formed a distinct ring-like structure (Figure 2, time points 4 min, 45 s onward), we detected astral microtubules interacting with and eventually converging at the medial cortex. As the asters interacted with the cortex, we also

*Correspondence: snejana@tll.org.sg

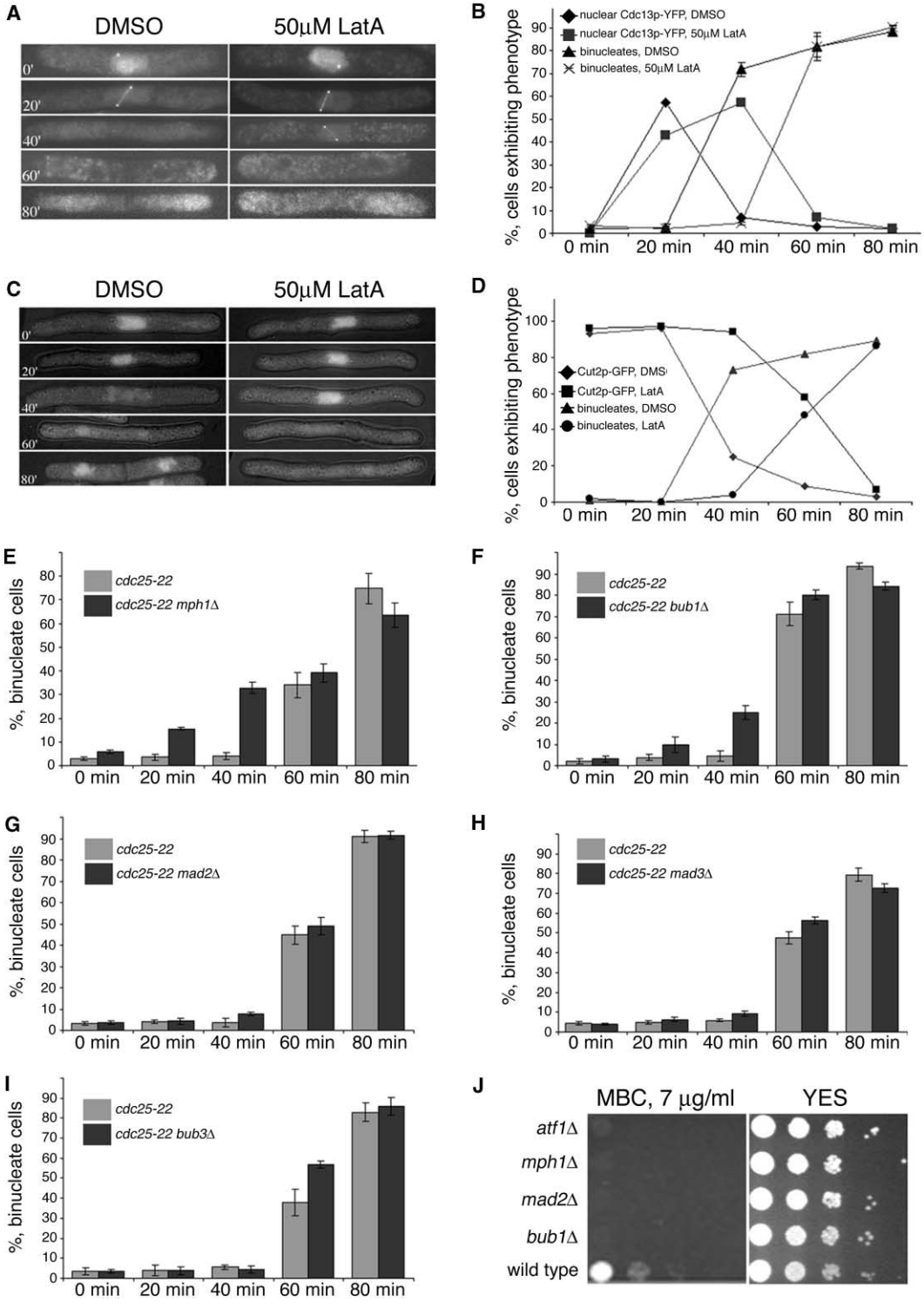

Figure 1. A Subset of SAC Components Functions to Monitor Defects in Spindle Orientation

(A) Cdc13p-YFP remains on all nuclear structures for the duration of LatA-induced metaphase arrest as shown in these YFP epifluorescence images of Cdc13p-YFP *cdc25-22* cells. Time refers to minutes after release to the permissive temperature of 24°C.

(B) Percentage of cells with Cdc13p-YFP on short spindles and percentage of binucleates in Cdc13p-YFP *cdc25-22* cells treated with 50 μM LatA or DMSO (n = 100 cells).

(C) Cut2p-GFP remains undestroyed during LatA-induced mitotic block.

(D–I) In (D), shown is the percentage of cells with nuclear securin and percentage of binucleates in Cut2p-GFP *cdc25-22* cells treated with 50 μM LatA or DMSO (n = 100 cells). Lack of either Mph1p (E) or Bub1p (F), but not Mad2p (G), Mad3p (H), or Bub3p (I), alleviated a delay in emergence of binucleate cells when *cdc25-22* cells treated with 50 μM LatA were synchronously released into mitosis (n = 500 cells for each time point).

(J) Serial dilutions of *atf1*Δ, *mph1*Δ, *mad2*Δ, *bub1*Δ, and wild-type cells were spotted on YES control plates and YES plates containing 7 μg/ml of methyl-1-(butylcarbamoyl)-2-benzimidizolecarbamate (MBC).

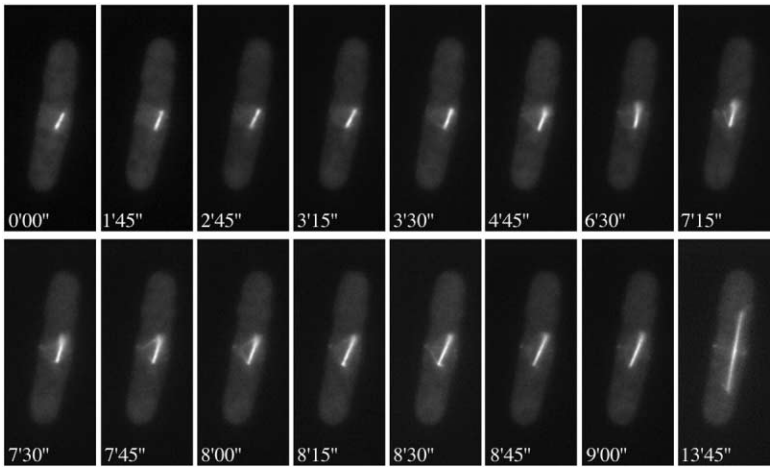

Figure 2. Astral Microtubules Converge at the Cortex Prior to Anaphase Onset

Time-lapse sequence of spindle and ring dynamics in wild-type cell expressing α-tubulin-EGFP and Rlc1p-EGFP. Numbers refer to the time (minutes and seconds) in the sequence.

observed the alignment of SPBs along the long axis of the cell (compare time points 3 min, 15 s through 6 min, 30 s). The spindle maintained constant length from time point 4 min, 45 s to time point 8 min, 00 s and initiated anaphase elongation at time point 8 min, 15 s. Anaphase movement thus appeared to be directly preceded by the convergence of astral microtubules at the medial cortex.

From analysis of time-lapse sequences, it appeared that upon interaction with the cortex, growing astral microtubules exerted physical force on the SPBs inducing their alignment. Hence, astral microtubules, the medial cortex, and the metaphase spindle could be represented as a mechanical system. The nuclear envelope is believed to be continuous with the cortical endoplasmic reticulum in fungi [17], anchoring the nucleus and providing a mechanical constraint on the system. It is apparent that aster-generated forces acting on the SPBs are strongest when the asters converge at the cortex and the spindle is aligned. Thus, an increase in the component of the force pushing the spindle poles apart could be predicted. Since the metaphase spindle maintains a nearly constant length [18–20], we hypothesized that a net increase in force production might lead to displacement of the SPB away from the spindle minus ends. Potentially, such displacement could be detected by a "sensor" molecule and signal to turn off the SOC.

In our model, such a molecule should form a connection between the SPB core and spindle microtubules and, preferably, possess structural features allowing it to act as a force transducer. Kendrin-like proteins are appealing candidates. They are conserved throughout evolution and are thought to connect centrosomal/SPB matrix to the minus ends of spindle microtubules [21–26]. Kilmartin and colleagues suggested that the central heptad repeat-rich coiled-coil region of the *Saccaromyces cerevisiae* kendrin Spc110p acts as a SPB/spindle spacer. Cells expressing ever larger in-frame deletions of this domain, exhibit decreasing distance between the spindle and the SPBs [21]. Thus, kendrins possess features that in principle could allow them to detect the displacement of SPBs with respect to spindle minus ends. In the absence of such a structural unit, spindle alignment should proceed normally, but the SOC would remain engaged.

Pcp1p (ORF SPAC6G9.06c) is a Spc110p/kendrin ortholog in *S. pombe* [24]. It is an essential protein exhibiting conservation of major structural features along the entire amino acid sequence with an exception of an extended N terminus [24]. In order to assess the potential role of Pcp1p's central coiled-coil domain in sensing spindle alignment, we replaced the wild-type copy of *pcp1*$^+$ with its in-frame deletion mutant *pcp1*Δ400-900 in which the coiled-coil domain, conserved between Spc110p and Pcp1p, was largely absent (Figure S2A). Cells containing *pcp1*Δ400–900 as a sole copy of the gene were viable and exhibited very few alterations in the microtubule cytoskeleton as described below. Strikingly, a major discernable phenotype was an enrichment of metaphase cells in an asynchronously growing population (Figure 3A). 11.2% ± 2.15% *pcp1*Δ400–900 cells exhibited short metaphase spindles and nonsegregated condensed chromosomes as compared to 2.1% ± 1.45% wild-type cells. Interestingly, metaphase spindles in *pcp1*Δ400–900 were slightly longer than wild-type: 2.51 ± 0.34 μm as compared to 2.01 ± 0.2 μm, respectively (n = 20). To confirm that *pcp1*Δ400–900 cells delayed in metaphase, we synchronously released these cells into mitosis using the *cdc25-22* temperature-sensitive mutation. *pcp1*Δ400–900 *cdc25-22* cells delayed in metaphase for approximately 15–20 min as compared to the *cdc25-22* control (Figure 3B). *pcp1*Δ400–900 cells with short spindles and nonsegregated chromosomes exhibited high levels of cyclin B, as judged by immunofluorescence analysis of *pcp1*Δ400-900 *cdc13*-YFP [9] cultures, consistent with their metaphase state (Figure 3C). A majority of short spindles in the *pcp1*Δ400–900 population were oriented with respect to the long axis of the cell: the mean angle of displacement was 19.9 ± 13.1° (n = 16), as compared to 16 ± 10.8° (n = 16) in wild-type, as previously determined [2]. Thus, *pcp1*Δ400-900 cells are delayed in metaphase with high levels of cyclin B and oriented spindles.

We then checked whether the metaphase delay experienced by *pcp1*Δ400–900 cells was SOC related. Introduction of either *mph1*$^+$ or *bub1*$^+$ deletions in the *pcp*1Δ400–900 background led to a drastic drop in the number of metaphase cells (2.1% ± 1.1% and 2.2% ± 1.8% respectively), bringing it to wild-type levels (Figure 3A). Additionally, deletion of *atf1*$^+$ in the *pcp1*Δ400–900

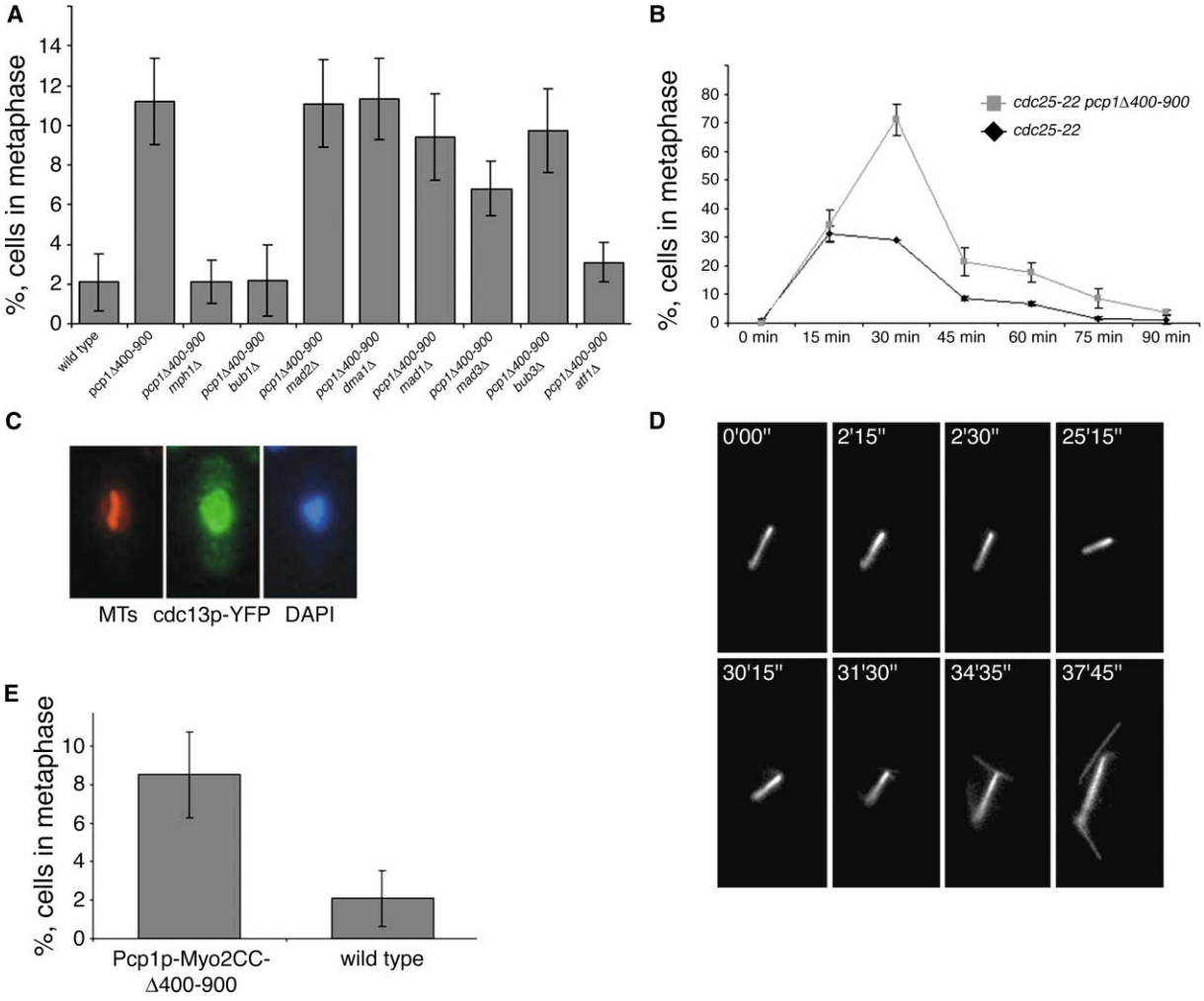

Figure 3. A Central Coiled-Coil Domain of Pcp1p Is Important for Sensing Spindle Orientation

(A) Percentage of metaphase cells in wild-type, *pcp1*Δ400-900, *pcp1*Δ400-900 *mph1*Δ, *pcp1*Δ400-900 *bub1*Δ, *pcp1*Δ400-900 *mad2*Δ, *pcp1*Δ400-900 *dma1*Δ, *pcp1*Δ400-900 *mad1*Δ, *pcp1*Δ400-900 *mad3*Δ, *pcp1*Δ400-900 *bub3*Δ, and *pcp1*Δ400-900 *atf1*Δ strains. Values are mean ± SD (n = 1000 cells).

(B) Synchronous release of *cdc25-22* and *pcp1*Δ400-900 *cdc25-22* cells from the G2 block shows that *pcp1*Δ400-900 are delayed in progression through metaphase (n = 500 for each time point).

(C) Immunofluorescence analysis of *pcp1*Δ400-900 *cdc13p*-YFP cells with short spindles confirms high cyclin B levels during this mitotic block.

(D) Time-lapse sequence of spindle dynamics in *pcp1*Δ400–900 cells expressing α-tubulin-EGFP. Numbers refer to the time (minutes and seconds) in the sequence.

(E) Percentage of metaphase cells in *pcp1-Myo2CC*-Δ400-900 cells as compared to wild-type. Values are mean ± SD (n = 1000 cells).

cells also alleviated the mitotic delay (Figure 3A). On the contrary, deletions of *mad2*$^+$, *mad1*$^+$, *bub3*$^+$, and *dma1*$^+$ [27] in the *pcp1*Δ400–900 background did not abolish the delay (Figure 3A), though the *pcp1*Δ400–900 *mad3*Δ double mutant exhibited a slight decrease in the number of metaphase cells (~7%).

Time-lapse analysis of spindle dynamics in *pcp1*Δ400–900 cells suggested that anaphase spindle elongation was delayed in spite of active spindle movements, multiple instances of astral microtubules/cortex interactions, and possibility of orienting the spindle (n = 20; Figure 3D and movie S2). Taken together, these data place the central coiled-coil domain of Pcp1p in the spindle orientation pathway and suggest that it might act as a structure that senses the achievement of proper alignment.

To answer whether this was a unique quality of the Pcp1p coiled-coil domain, we checked whether domains with somewhat similar secondary structures could substitute for its function. We generated a strain (*pcp1-Myo2CC*-Δ400–900) in which the coiled-coil domain of Pcp1p was replaced by a part of the C-terminal coiled-coil domain of the type II myosin Myo2p (amino acids 900–1351) (Figure S2B). Myo2p C-terminal coiled-coil was proposed to form a rod-like structure [28], a property similar to that of the Spc110p coiled-coil [21]. The mitotic phenotype of an asynchronously growing *pcp1-Myo2CC*-Δ400–900 cell population was compara-

ble to that of the *pcp1*Δ400–900 strain. Not only was there an increased percentage of metaphase cells as compared to the control (Figure 3E), but we also observed an increase in mean metaphase spindle length (2.46 ± 0.40 μm, n = 20). Spindle orientation in *pcp1-Myo2CC*-Δ400–900 cells occurred normally as the mean angle of displacement of metaphase spindles was comparable to wild-type (18.6 ± 12.1°, n =16). Thus, it is not simply a coiled-coil rod-like structure, but a certain primary amino acid sequence encoding specific structural features that could be important for detecting spindle alignment.

In conclusion, our experiments indicate that a subset of SAC components monitors alignment of the metaphase spindle in fission yeast. They also implicate that the kendrin-like SPB protein Pcp1p functions in this process. We would like to suggest that the central coiled-coil domain of Pcp1p might detect a net increase in force developing at the SPBs upon spindle orientation and signal to disengage the SOC. An exciting possibility would be if such a structure could undergo a certain degree of conformational change upon spindle alignment, resulting either in binding of a distinct set of regulatory proteins or directly influencing the γ-tubulin organizing function of its N terminus. Interestingly, this domain contains several regions breaking the coiled-coil structure [29], which might contribute to flexibility and elasticity of the protein. How does this protein domain function during spindle orientation? How could it signal to Mph1p and Bub1p to regulate this process? In the bifurcation model of the SAC, with distinct signals monitoring kinetochore attachment and tension across the spindle, both Mph1p and Bub1p are thought to execute the tension-sensing events of the checkpoint [30]. Could these proteins function in sensing tension at the spindle poles? We hope to address these and related questions in our future experiments.

Supplemental Data

Supplemental Data including additional experiments on cell cycle delay in cells treated with latA and latB, experimental procedures, and time-lapse movies in QuickTime format are available at http://www.current-bioogy.com/cgi/content/full/14/1/69/DC1/.

Acknowledgments

S. Jesuthasan and D. Pellman kindly corrected the manuscript. Conversations with several colleagues, in particular F. Uhlmann, D. McCollum, S. Naqvi and V. Wachtler have been extremely helpful for this project. We are grateful to K. Gull, Y. Hiraoka, D. McCollum, J. Millar, M. Yanagida and A. Decottignies for generous sharing of materials and reagents. This work was supported by intramural funds from the Temasek Life Sciences Laboratory.

Received: July 21, 2003
Revised: October 7, 2003
Accepted: November 19, 2003
Published: January 6, 2004

References

1. Gachet, Y., Tournier, S., Millar, J.B., and Hyams, J.S. (2001). A MAP kinase-dependent actin checkpoint ensures proper spindle orientation in fission yeast. Nature *412*, 352–355.
2. Oliferenko, S., and Balasubramanian, M.K. (2002). Astral microtubules monitor metaphase spindle alignment in fission yeast. Nat. Cell Biol. *4*, 816–820.
3. Geldmacher-Voss, B., Reugels, A.M., Pauls, S., and Campos-Ortega, J.A. (2003). A 90-degree rotation of the mitotic spindle changes the orientation of mitoses of zebrafish neuroepithelial cells. Development *130*, 3767–3780.
4. Cayouette, M., and Raff, M. (2003). The orientation of cell division influences cell-fate choice in the developing mammalian retina. Development *130*, 2329–2339.
5. Kaltschmidt, J.A., Davidson, C.M., Brown, N.H., and Brand, A.H. (2000). Rotation and asymmetry of the mitotic spindle direct asymmetric cell division in the developing central nervous system. Nat. Cell Biol. *2*, 7–12.
6. Carminati, J.L., and Stearns, T. (1997). Microtubules orient the mitotic spindle in yeast through dynein-dependent interactions with the cell cortex. J. Cell Biol. *138*, 629–641.
7. Yin, H., Pruyne, D., Huffaker, T.C., and Bretscher, A. (2000). Myosin V orientates the mitotic spindle in yeast. Nature *406*, 1013–1015.
8. Liakopoulos, D., Kusch, J., Grava, S., Vogel, J., and Barral, Y. (2003). Asymmetric loading of Kar9 onto spindle poles and microtubules ensures proper spindle alignment. Cell *112*, 561–574.
9. Decottignies, A., Zarzov, P., and Nurse, P. (2001). In vivo localisation of fission yeast cyclin-dependent kinase cdc2p and cyclin B cdc13p during mitosis and meiosis. J. Cell Sci. *114*, 2627–2640.
10. Rupes, I., Webb, B.A., Mak, A., and Young, P.G. (2001). G2/M arrest caused by actin disruption is a manifestation of the cell size checkpoint in fission yeast. Mol. Biol. Cell *12*, 3892–3903.
11. Kumada, K., Nakamura, T., Nagao, K., Funabiki, H., Nakagawa, T., and Yanagida, M. (1998). Cut1 is loaded onto the spindle by binding to Cut2 and promotes anaphase spindle movement upon Cut2 proteolysis. Curr. Biol. *8*, 633–641.
12. Sato, M., Koonrugsa, N., Toda, T., Vardy, L., Tournier, S., and Millar, J.B. (2003). Deletion of Mia1/Alp7 activates Mad2-dependent spindle assembly checkpoint in fission yeast. Nat. Cell Biol. *5*, 764–766.
13. Oliferenko, S., and Balasubramanian, M.K. (2003). Reply: deletion of Mia1/Alp7 activates Mad2-dependent spindle assembly checkpoint in fission yeast. Nat. Cell Biol. *5*, 766.
14. Ding, D.Q., Chikashige, Y., Haraguchi, T., and Hiraoka, Y. (1998). Oscillatory nuclear movement in fission yeast meiotic prophase is driven by astral microtubules, as revealed by continuous observation of chromosomes and microtubules in living cells. J. Cell Sci. *111*, 701–712.
15. Naqvi, N.I., Wong, K.C., Tang, X., and Balasubramanian, M.K. (2000). Type II myosin regulatory light chain relieves auto-inhibition of myosin-heavy-chain function. Nat. Cell Biol. *2*, 855–858.
16. Le Goff, X., Motegi, F., Salimova, E., Mabuchi, I., and Simanis, V. (2000). The S. pombe rlc1 gene encodes a putative myosin regulatory light chain that binds the type II myosins myo3p and myo2p. J. Cell Sci. *113*, 4157–4163.
17. Pidoux, A.L., and Armstrong, J. (1993). The BiP protein and the endoplasmic reticulum of Schizosaccharomyces pombe: fate of the nuclear envelope during cell division. J. Cell Sci. *105*, 1115–1120.
18. Li, X., and Nicklas, R.B. (1995). Mitotic forces control a cell-cycle checkpoint. Nature *373*, 630–632.
19. Tanaka, T., Fuchs, J., Loidl, J., and Nasmyth, K. (2000). Cohesin ensures bipolar attachment of microtubules to sister centromeres and resists their precocious separation. Nat. Cell Biol. *2*, 492–499.
20. Mallavarapu, A., Sawin, K., and Mitchison, T. (1999). A switch in microtubule dynamics at the onset of anaphase B in the mitotic spindle of Schizosaccharomyces pombe. Curr. Biol. *9*, 1423–1426.
21. Kilmartin, J.V., Dyos, S.L., Kershaw, D., and Finch, J.T. (1993). A spacer protein in the Saccharomyces cerevisiae spindle pole body whose transcript is cell cycle-regulated. J. Cell Biol. *123*, 1175–1184.
22. Tassin, A.M., Celati, C., Paintrand, M., and Bornens, M. (1997). Identification of an Spc110p-related protein in vertebrates. J. Cell Sci. *110*, 2533–2545.
23. Flory, M.R., Moser, M.J., Monnat, R.J., Jr., and Davis, T.N. (2000). Identification of a human centrosomal calmodulin-bind-

ing protein that shares homology with pericentrin. Proc. Natl. Acad. Sci. USA *97*, 5919–5923.
24. Flory, M.R., Morphew, M., Joseph, J.D., Means, A.R., and Davis, T.N. (2002). Pcp1p, an Spc110p-related calmodulin target at the centrosome of the fission yeast Schizosaccharomyces pombe. Cell Growth Differ. *13*, 47–58.
25. Nguyen, T., Vinh, D.B., Crawford, D.K., and Davis, T.N. (1998). A genetic analysis of interactions with Spc110p reveals distinct functions of Spc97p and Spc98p, components of the yeast gamma-tubulin complex. Mol. Biol. Cell *9*, 2201–2216.
26. Spang, A., Grein, K., and Schiebel, E. (1996). The spacer protein Spc110p targets calmodulin to the central plaque of the yeast spindle pole body. J. Cell Sci. *109*, 2229–2237.
27. Murone, M., and Simanis, V. (1996). The fission yeast dma1 gene is a component of the spindle assembly checkpoint, required to prevent septum formation and premature exit from mitosis if spindle function is compromised. EMBO J. *15*, 6605–6616.
28. Bezanilla, M., and Pollard, T.D. (2000). Myosin-II tails confer unique functions in Schizosaccharomyces pombe: characterization of a novel myosin-II tail. Mol. Biol. Cell *11*, 79–91.
29. Lupas, A., Van Dyke, M., and Stock, J. (1991). Predicting coiled coils from protein sequences. Science *252*, 1162–1164.
30. Zhou, J., Yao, J., and Joshi, H.C. (2002). Attachment and tension in the spindle assembly checkpoint. J. Cell Sci. *115*, 3547–3555.